

Lawrence Berkeley National Laboratory

Recent Work

Title

EFFECTS OF OFF-MASS-SHELL CONTINUATION IN THE MULTIPERIPHERAL MODEL

Permalink

<https://escholarship.org/uc/item/1th5j909>

Author

Avalos, Daniel R.

Publication Date

1971-08-01

Submitted to Physical Review

LBL-44
Preprint

ca

RECEIVED
RADIATION LABORATORY

14

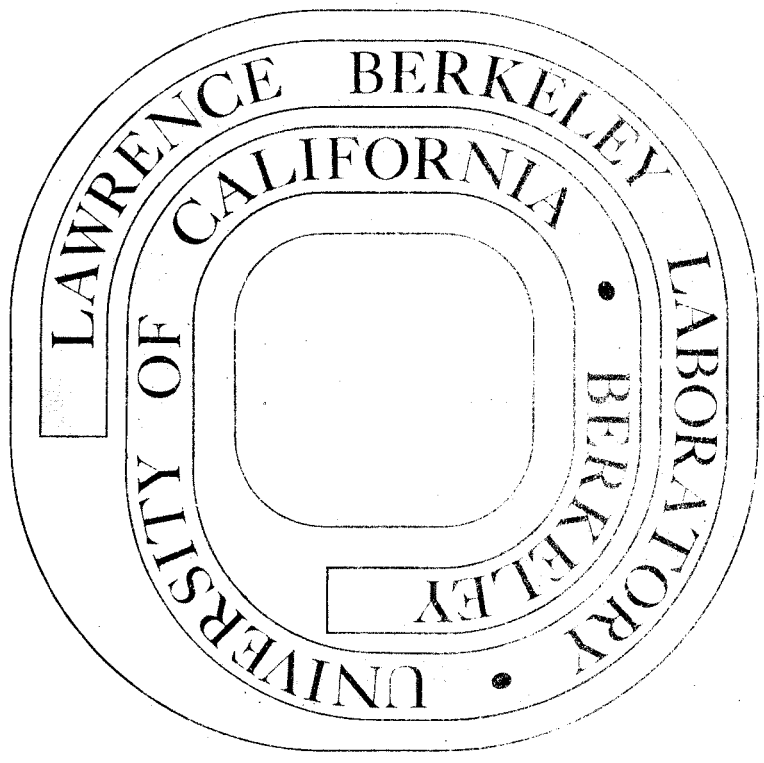
DOCUMENTS SECTION

EFFECTS OF OFF-MASS-SHELL CONTINUATION IN
THE MULTIPERIPHERAL MODEL

Daniel R. Avalos and Bryan R. Webber

August 20, 1971

AEC Contract No. W-7405-eng-48



TWO-WEEK LOAN COPY
This is a Library Circulating Copy
which may be borrowed for two weeks.
For a personal retention copy, call
Tech. Info. Division, Ext. 5545

34a

LBL-44

ca

DISCLAIMER

This document was prepared as an account of work sponsored by the United States Government. While this document is believed to contain correct information, neither the United States Government nor any agency thereof, nor the Regents of the University of California, nor any of their employees, makes any warranty, express or implied, or assumes any legal responsibility for the accuracy, completeness, or usefulness of any information, apparatus, product, or process disclosed, or represents that its use would not infringe privately owned rights. Reference herein to any specific commercial product, process, or service by its trade name, trademark, manufacturer, or otherwise, does not necessarily constitute or imply its endorsement, recommendation, or favoring by the United States Government or any agency thereof, or the Regents of the University of California. The views and opinions of authors expressed herein do not necessarily state or reflect those of the United States Government or any agency thereof or the Regents of the University of California.

EFFECTS OF OFF-MASS-SHELL CONTINUATION IN
THE MULTIPERIPHERAL MODEL *

Daniel R. Avalos[†] and Bryan R. Webber[‡]

Lawrence Berkeley Laboratory
University of California
Berkeley, California 94720

August 20, 1971

ABSTRACT

The predictions of the Amati-Bertocchi-Fubini-Stanghellini-Tonin multiperipheral model concerning Regge trajectories and residues are presented for a number of different parametrizations of the off-shell $\pi\pi$ scattering amplitude. The unmodified model, in which the kernel is taken to be the on-shell amplitude, gives unsatisfactory results. The most natural continuation appears to involve the phenomenological form factors of Dür and Pilkuhn (DP). The use of the DP factors leads to trajectories with slope about 1 GeV^{-2} and intercepts $\alpha_{I=0} = 0.57$ and $\alpha_{I=1} = 0.36$. When K and η meson exchange are included in the model, the DP factors provide a sensible way of including bound-state vertices such as $\rho K\bar{K}$ and $K^* K\eta$. The trajectory intercepts are now increased to $\alpha_{I=0} = 0.63$ and $\alpha_{I=1} = 0.42$, and the average multiplicities of the various secondaries are of the form $c \ln s$, where $c_\pi = 0.84$, $c_K = 0.11$,

$c_\eta \approx 10^{-4}$. It seems possible that this model, in conjunction with the "schizophrenic Pomeranchon" mechanism, can provide a good description of high-energy processes.

I. INTRODUCTION

Several recent papers¹⁻⁵ have investigated the quantitative predictions of the pion-exchange multiperipheral model originally proposed by Amati et al. in 1962 (the ABFST model).⁶ In order to summarize these predictions, it is convenient to divide them into two classes. First, there is a class of predictions concerning spectra and multiplicities of secondaries in multiparticle production processes. These appear generally to be in good agreement with experiment: for example, the coefficient of the logarithmic increase of multiplicity with energy is roughly correct,^{1,7} and the transverse momentum spectrum of secondary pions has the observed form.⁸

The second class of predictions concerns the absorptive parts of high-energy elastic amplitudes, which are calculated by imposing unitarity in the form of the ABFST integral equation. Since the model in its unmodified form leads to amplitudes that are asymptotically dominated by Regge poles, these predictions may be discussed in terms of Regge trajectories and their residues. Up to now, only the intercepts of the vacuum and ρ trajectories have been calculated.¹ These are in poor agreement with experiment: the intercepts are given as about 0.30 and 0.14, respectively, whereas the true intercepts are about 1.0 and 0.5.

By the "unmodified" form of the ABFST model we mean the form in which the kernel of the integral equation is taken to be the on-mass-shell, low-energy absorptive part of the $\pi\pi$ scattering amplitude: in practice, this kernel is taken to be saturated by a few narrow resonances.

In this article we first present, in Sec II, the predictions of the unmodified model concerning the Regge trajectories and residues at nonzero (negative) values of t . The behavior of the trajectories at nonzero t is found to be even less satisfactory than that at $t = 0$. Some modification of the model is clearly required if it is to give more realistic results.

Various authors have considered the modification of the model to include: (a) interference terms;^{3,5} (b) other channels, such as $K\bar{K}$ and $\eta\eta$;⁹ (c) the contribution of high-energy $\pi\pi$ scattering in the kernel;^{2,10} (d) off-mass-shell continuation of the $\pi\pi$ amplitude.^{1,5} Apart from the off-shell continuation all these modifications are non-controversial and lead to slight improvements in the model, that is, to small increases in the predicted trajectory intercepts. However, we shall argue that the most important and necessary modification must involve an off-shell continuation, and our principal aim in this article is to investigate what we believe to be the most natural form of continuation, namely, the use of phenomenological Dürr-Pilkuhn¹¹ (DP) form factors.

A number of possible off-shell continuations have been discussed by Tow,¹ who concluded that they would not lead to improvements in the predictions of the model. However, all the continuations considered by Tow involved drastic changes in the asymptotic behavior of the $\pi\pi$ amplitude, which led either to a decrease in the kernel strength or to undesirable increases in the average momentum transfer. The DP form factors, on the other hand, are asymptotically constant, and give rise to a general overall increase in the kernel strength without making fundamental changes in the form of the amplitude.

In Sec. III we discuss the DP form factors in more detail and apply them to the ABFST model. The results suggest that this modification of the model, in conjunction with the other improvements listed above, will provide a much better description of high-energy processes. In particular we go on in Sec. IV to discuss the effect of including the $\bar{K}\bar{K}$ and $\eta\eta$ channels in addition to the DP factors. In this application, the DP factors have the further advantage of giving a well-defined and sensible prescription for the inclusion of bound-state vertices, such as $\rho\bar{K}\bar{K}$ and $K^*K\eta$. The effect of the extra channels is found to be enhanced by the form factors, although little of the enhancement is due to the bound states.

We discuss the probable effects of further modifications of the model, and form some conclusions, in Sec. V.

II. SUMMARY OF PREDICTIONS OF THE UNMODIFIED MODEL

The ABFST model is defined by the integral equation shown in Fig. 1, which represents the hypothesis that the total $\pi\pi$ absorptive part is obtained by iteration of the low-energy contribution. Corresponding to the various four-momenta defined in Fig. 1, we define the invariants:

$$\begin{aligned} s &= (k - k')^2, & s_0 &= (k - k'')^2, & t &= p^2, \\ u &= -k^2, & u' &= -k'^2, & u'' &= -k''^2. \end{aligned} \quad (2.1)$$

In the forward-scattering case ($t = 0$), the equation may be written in the form:¹²

$$A_\lambda(u, u') = A_\lambda^R(u, u') + \frac{1}{16\pi^3(\lambda + 1)} \int_0^\infty du'' \frac{A_\lambda^R(u, u'') A_\lambda(u'', u')}{(u'' + m_\pi^2)^2}, \quad (2.2)$$

which has been diagonalized by means of the Laplace transform

$$A_\lambda(u, u') = \int_0^\infty ds e^{-(\lambda+1)\eta(s, u, u')} A(s; u, u'), \quad (2.3)$$

where

$$\eta(s, u, u') = \cosh^{-1} \left(\frac{s + u + u'}{2(uu')^{\frac{1}{2}}} \right), \quad (2.4)$$

and $A(s; u, u')$ is the forward absorptive part. Similarly, $A^R(s; u, u')$ is the low-energy absorptive part and $A_\lambda^R(u, u')$ is its Laplace transform. We shall assume that $A^R(s; u, u')$ can be expressed as a sum over narrow resonances i ($i = \epsilon, \rho, f, f', \text{ and } g$); that is,

$$A^R(s; u, u') = 2\pi \sum_i \beta_i g_i^2 F_i^2(q_{\text{off}}) \delta(s - m_i^2), \quad (2.5)$$

where β_i is the isospin crossing matrix element appropriate to resonance i and the t -channel isospin state being considered, and

$$g_i^2 = 16\pi(2J_i + 1) m_i^2 \Gamma_i x_i / \lambda^{\frac{1}{2}}(m_i^2, m_\pi^2, m_\pi^2), \quad (2.6)$$

where

$$\lambda(a, b, c) = a^2 + b^2 + c^2 - 2ab - 2ac - 2bc, \quad (2.7)$$

and J_i , Γ_i , and x_i are the spin, width, and elasticity of the resonance. In (2.5) $F_i(q_{\text{off}})$ is the form factor for the $i\pi\pi$ vertex, normalized such that

$$F_i(q_{\text{on}}) = 1,$$

where q_{on} (q_{off}) is the on-shell (off-shell) c.m. momentum for the vertex:

$$q_{\text{on}} = \lambda^{\frac{1}{2}}(s, m_\pi^2, m_\pi^2) / [2(s)^{\frac{1}{2}}],$$

and

$$q_{\text{off}} = \lambda(s, -u, -u') / [2(s)^{\frac{1}{2}}]. \quad (2.8)$$

In the unmodified model, one sets

$$F_i(q_{\text{off}}) \equiv 1. \quad (2.9)$$

The variable λ in Eqs. (2.2) and (2.3) is the usual parameter of the $O(3,1)$ group representations;¹³ when $A_\lambda(u, u')$ has a pole in the λ plane, there is an associated family of Regge poles at

$$\alpha = \lambda, \lambda - 2, \lambda - 4, \dots$$

When Eq. (2.2) is generalized to nonforward scattering ($t \neq 0$), the full $O(3,1)$ symmetry is not preserved and there is a coupling between equations involving different values of λ . The extra complications of the nonforward equation may be found in the Appendix, together with a discussion of the method and approximations used in its solution. The important point to note here is that the kernel of the unmodified nonforward equation involves the on-shell low-energy absorptive part: corresponding to Eqs. (2.5) and (2.9) we have in this case

$$\begin{aligned} A^R(s, t; u, u') &= A^R(s, t; -m_\pi^2, -m_\pi^2) \\ &= 2\pi \sum_i \beta_i g_i^2 \delta(s - m_i^2) P_{J_i} \left(1 + \frac{t}{2q_{\text{on}}^2} \right). \end{aligned} \quad (2.10)$$

The set of resonances that we used consisted of the first five states listed in Table I. The assumed properties of these resonances are indicated in Tables I and II. After inserting the kernel (2.10) into (A.2), we may solve the integral equation numerically to obtain the leading $I = 0$ and $I = 1$ Regge trajectories and their residues; these are shown by the dashed curves in Figs. 2 and 3.

The trajectory intercepts in Fig. 2 agree with those found in previous solutions¹ of the forward ABFST equation, and they are too small to correspond with experimental observations. The trajectory slopes, on the other hand, are much too large: the Regge poles plunge down to $\ell = -1$ at $t \approx -0.35 \text{ GeV}^2$, and for more negative t they move off into the complex ℓ plane. The reason for this strange behavior is that the kernel of the integral equation changes sign at $t \approx -0.35 \text{ GeV}^2$, because all the Legendre polynomials in Eq. (2.10)

(except the small $J = 0$ contribution of the ϵ) have zeros near this point.

The Regge residues shown in Fig. 3 are defined in such a way that the imaginary part of the amplitude with the corresponding t -channel isospin is given by

$$A(s, t; u, u') \sim \gamma(t; u, u') (s/s_0)^{\alpha(t)}, \quad (2.11)$$

where

$$\beta(t) \equiv \gamma(t; -m_\pi^2, -m_\pi^2)$$

and $s_0 = 1 \text{ GeV}^2$. The values and logarithmic derivatives of the residue functions at $t = 0$ are of the correct order of magnitude, but are slightly too large: experimentally, one finds $\beta_{I=0}(0) \approx 100$, $\beta_{I=1}(0) \approx 40$, $d(\ln \beta_{I=0,1})/dt \approx 5 \text{ GeV}^{-2}$. As in the case of the Regge trajectories, there is unphysical behavior near $t \approx -0.35 \text{ GeV}^2$ owing to the change of sign of the kernel function.

Several authors^{14,15} have avoided the introduction of zeros into the ABFST kernel by treating the $\pi\pi$ resonances as scalar particles [except in the statistical weight factor $(2J_1 + 1)$]. This has the effect of removing the Legendre polynomials from Eq. (2.10), which changes the Regge trajectories and residues to those shown by the dotted curves in Figs. 2 and 3. It is hard to see how such a procedure can be justified in terms of the original ABFST prescription of using the on-shell low-energy $\pi\pi$ amplitude as the kernel. In any case, the trajectories and residues, although no longer singular at negative t , are now too flat to agree with experiment: the residue functions, for example, have negative derivatives at $t = 0$.

The treatment of the $\pi\pi$ resonances as scalars might be regarded as equivalent to an off-mass-shell continuation that eliminates the t -dependence of the kernel. A more natural continuation would involve the use of the off-shell expression for $\cos \theta_s$, given in the Appendix by Eq. (A.6), as the argument of the Legendre polynomials in Eq. (2.10). This prescription adjusts the t -dependence to preserve the angular momentum structure of the amplitude when it is taken off-shell. The trajectories and residues for this continuation are shown by the dot-dashed curves in Figs. 2 and 3. There is considerable improvement over both the on-shell and scalar-resonance results: the trajectory slopes are about 1 GeV^{-2} , and the residue functions have positive logarithmic derivatives.

Of course, all the prescriptions we have considered so far give the same unsatisfactory trajectory intercepts, because they are all equivalent at $t = 0$. Another result that follows from the forward equation alone concerns the average multiplicity of secondaries in high-energy inelastic collisions. This is predicted to increase like $c \ln s$, where $c = 0.74$ in the unmodified ABFST model,¹ which is in fair agreement with experimental observations, as shown in Table III.

A problem with all the above treatments of the nonforward ABFST equation is that a tachyon (that is, a particle with negative mass-squared) is generated at the point where $\alpha_{I=0} = 0$. However, in the case of the dot-dashed curves in Figs. 2 and 3, corresponding to the "off-shell $\cos \theta_s$ " prescription, it seems possible that some small perturbation could produce the zero in the residue function that is required to remove the tachyon pole.

III. INCLUSION OF DÜRR-PILKUHN FORM FACTORS

Instead of looking at the results of the unmodified ABFST model as a failure of the pion-exchange hypothesis, we prefer to emphasize here the point that the ABFST equation is an equation for the off-shell amplitude, so that we have to use a reasonable off-shell amplitude as input before we start looking for refinements to the model. As we stated before, our aim is to investigate the off-shell continuation given by the phenomenological DP form factors.

The reasons for preferring this kind of continuation are briefly as follows: it gives the correct threshold behavior; it behaves asymptotically like the on-shell amplitude, thus introducing no fundamental changes in its functional form; it permits a straightforward generalization to bound state scattering; and it has been recently used extensively, and successfully, in fitting data on single-pion-exchange reactions.¹⁶

Furthermore, as Dürr¹⁷ has pointed out, the DP form factors are to be regarded as being kinematic factors which account for centrifugal barrier effects that are known to be present.

For the meson vertex, the DP factors are of the general form:¹¹

$$F_i(q_{\text{off}}) = \left[\frac{v_\ell(q_{\text{off}} R)}{v_\ell(q_{\text{on}} R)} \right]^{\frac{1}{2}}, \quad (3.1)$$

where

$$v_\ell(x) = \{x^2 [j_\ell^2(x) + n_\ell^2(x)]\}^{-1}; \quad (3.2)$$

the partial wave being given by $\ell = J_i$, and j_ℓ and n_ℓ being the spherical Bessel and Neumann functions.

The expressions for q_{on} and q_{off} are given by Eq. (2.8), or (A.5), and the radius R (one for each resonance) is a parameter to be determined by fitting experimental data.

A problem one faces immediately with this kind of off-shell continuation is the assignment of reasonable values to the parameters R . This is so because they are poorly determined by experiment and in general are known only within an order of magnitude. It becomes clear that in order to avoid a model with many free parameters some criteria must be used to give values to them.

Since R is best known for p-waves, we have assigned to $R_{\rho\pi\pi}$ the value given by experimental fits, and have adjusted the remaining R 's by requiring that the corresponding form factors satisfy the condition that

$$\langle r^2 \rangle_i = -6 \frac{\partial F_i}{\partial u} \Big|_{u=-\frac{m_\pi^2}{\pi}} \quad (3.3)$$

be independent of i . That is, following Wolf¹⁸ we define a rms "radius of interaction" and require that it be the same for all partial waves.

Table II gives the values of R used in the present work. The corresponding $\langle r^2 \rangle^{\frac{1}{2}}$ of $0.4F$ is slightly smaller than the value of about $0.6F$ recommended by Wolf. In passing, we note that due to the different momenta and form factors involved for each value of ℓ , the R 's are very different from one another.

The value of $R_{\rho\pi\pi}$ is the one quoted in Ref. 19, and it happens to be the same one necessary to get fairly good agreement between $SU(3)$ predictions and the experimental decay widths of vector mesons.²⁰

The remaining R 's computed according to Eq. (3.3) are consistent with values given in the literature.²¹

After substituting Eq.(3.2) into Eq. (3.1) for each resonance, and inserting the resulting expression in the kernel, Eq. (A.4), we once more solved the integral equation numerically, obtaining the trajectories and residues shown by solid curves in Figs. 2 and 3.

We see that the main effect of the DP factors (relative to the "off-shell $\cos \theta_s$ " curve) amounts to an overall change in normalization, leaving the general shape of the trajectories and residues almost unchanged—a desirable feature in view of the uncertainties in the values of the parameters R . Furthermore, one notes that refinements of the model [for example, taking full account of the $O(3,1)$ -symmetry-breaking terms--see Appendix] might produce a zero in the residue function in the correct place to remove the tachyon pole. The values of the residues at $t = 0$ seem to be too large, although they are in a ratio in close agreement with experiment (see Sec. II). The logarithmic derivatives of the residues have the reasonable value of about 1.25 GeV^{-2} . The average multiplicity of secondaries is now improved, and is given by

$$\langle n \rangle = 0.84 \ln s + \text{const.} , \quad (3.5)$$

which is still somewhat smaller than the experimental value.

It is also of interest to mention the effect of the DP form factors on the transverse momentum distribution of secondaries. It has been shown that within the framework of the ABFST model, this is insensitive to the details of the off-shell low-energy scattering amplitudes,⁸ being a rather constant property of the model which is in good agreement with experiment. It is the normalization of the

distribution (which is related to the average multiplicity) that depends on the detailed structure of the low-energy amplitudes, and it is found in this case that the DP prescription is the one that gives the best results.

From the preceding discussion we conclude that the DP form factors do improve the quantitative predictions of the model. One question that arises naturally concerns the combined effect of including K and η exchange together with DP form factors in the kernel. We examine this in the next section.

IV. INCLUSION OF K AND η EXCHANGE

The formalism we used in the generalization of the ABFST model to include K and η exchange has been detailed elsewhere.⁹ In this case, however, it remains to specify the values of the parameters used: these are given in Table II.

Once again we applied Eq. (3.3), using a rms radius of $0.4F$ for the KK resonances but the slightly smaller value of $0.3F$ for the $K\pi$ channel. We kept the value of $0.4F$ unchanged for the KK channel because it yields values of R for that vertex that are consistent with experimental fits.²²

For the $K\pi$ system the situation is complicated by the fact that the only reported fits have been made using a modified propagator for the pion. Nevertheless, Trippe et al.²³ have found that a smaller rms radius is needed to describe the data for the $K\pi$ state than that used in the $\pi\pi$ case, and accordingly we reduced the value of the interaction radius slightly in this case.

The kernel is now built up from all the resonances listed in Table I.

Apart from resonant states, we have included the ρ and ω as bound state poles of the $K\bar{K}$ system, and similarly the K^* as a pole in the $K\eta$ channel. We evaluated the corresponding coupling constants in an $SU(3)$ -symmetric fashion. As we pointed out before, the DP factors make the inclusion of such states a straightforward matter: in the place of the factor $g_i^2 F_i^2(q_{\text{off}})$ in Eq. (2.5) one has now a factor $G_i^2 v_\ell(q_{\text{off}} R)$, where G_i is the $SU(3)$ -symmetric coupling constant.

To keep the problem within manageable proportions we computed only the $t = 0$ intercepts of the resulting nonstrange t -channel $I = 0$ and $I = 1$ trajectories and the average multiplicity of produced secondaries. The results are those shown in Table III.

The main thing to note here is that the effect of K and η exchange is now fairly important, its contribution being twice as large as in the on-shell calculation. The intercepts of both trajectories are raised by roughly the same amount of 0.06 . Furthermore, this increase is due almost entirely to K exchange. The exchange of η 's gives a contribution that is, at most, one order of magnitude smaller than that of K exchange. This is also the order of magnitude of the contribution of the three bound states mentioned above.

The average multiplicity (see Table III) shows considerable improvement too, being in good agreement with recent experimental findings.⁷

The different secondaries are in the ratio

$$[\langle n_K \rangle / \langle n_\pi \rangle] \sim 0.13 \quad (4.1)$$

with negligible η production ($\langle n_\eta \rangle \approx 10^{-4} \ln s + \text{const.}$). To find the multiplicity of secondaries, we first computed the multiplicity of each final (i.e., resonant) state in the usual way,⁶ and then we obtained the multiplicity of secondaries by multiplying by the experimental decay widths of the states.

The ratio between the couplings of the vacuum pole to the $\pi\pi$ channel, $\beta_\pi(0)$, and to the $K\bar{K}$ system, $\beta_K(0)$, was also estimated. From factorization and the known values of K^+p and π^+p total cross sections one would expect this ratio to be of the order of

$$\xi \equiv [\beta_{\pi}(0)/\beta_K(0)] \approx 1.6-1.7, \quad (4.2)$$

where due account has been taken of crossing matrix factors. Our value,

$$\xi \approx 1.8, \quad (4.3)$$

compares well with experiment.

Finally, the ABFST eigenfunction,⁶ $\Phi(u)$, given in the notation of Eq. (2.11) by

$$\Phi(u) \equiv \gamma(0; u, -m_{\pi}^2), \quad (4.4)$$

was also evaluated. It appeared to be remarkably constant over a large interval of u , especially in the important region: $0 \leq u \leq 0.1$. In Fig. 4 we show the behavior of $\Phi^{\pi\pi}(u)$, $\Phi^{\pi K}(u)$, and $\Phi^{\pi\eta}(u)$, with arbitrary total normalization.

V. CONCLUSIONS

We have shown that the original ABFST model, in which the kernel is taken to be the on-shell low-energy $\pi\pi$ absorptive part, must be modified to include an off-shell continuation if the output Regge trajectories are to have acceptable behavior at negative values of t . A continuation based on the Dürr-Pilkuhn form factors gives improved results, and does not seem to interfere with any of the good predictions of the model. In fact, it brings the predicted multiplicities of secondaries into better agreement with experimental results. The behavior of the residue functions at large negative t remains unsatisfactory (in particular, there is a tachyon pole in the isoscalar amplitude at $t = -1.1 \text{ GeV}^2$), but perhaps one should not believe a multiperipheral model at such large momentum transfers, even if some additional perturbation is sufficient to improve the residue behavior.

When K and η meson exchange are included in the model, it gives leading trajectory intercepts $\alpha_{I=0} = 0.63$ and $\alpha_{I=1} = 0.42$. Although the intercept of the isovector trajectory is now large enough for it to be identified with the ρ , the isoscalar trajectory is still too low to be called the Pomeranchon. However, its properties now make it a good candidate for the degenerate leading trajectory discussed by Chew and Snider in their "schizophrenic Pomeranchon" model.¹⁰ Such a trajectory would split into two components (corresponding to the P and P') under the influence of a J -plane branch point associated with the small high-energy component of the $\pi\pi$ scattering amplitude. In order to split into P and P' poles with the observed properties, the degenerate trajectory should have $\alpha(0) \approx 0.7$, $\alpha' \approx 1 \text{ GeV}^{-2}$, and $\beta(0) \approx 200$. The vacuum trajectory that we have calculated does in fact have very nearly these properties. Thus we expect that the

inclusion of a high-energy component in the ABFST kernel, in addition to the low-energy resonance with DP factors, will produce a pair of output vacuum trajectories that are very similar to the physical P and P' trajectories. Provided the ρ trajectory is not strongly split by a similar mechanism, one would expect approximate degeneracy of the resulting P' and ρ trajectories and residue functions.

There is a certain lack of elegance in the hypothesis that a variety of apparently unrelated small effects ($\pi\pi$ resonances, off-shell continuation, K and η exchange, and the schizophrenic mechanism) combine to give a Pomeranchuk intercept near unity, but it does seem increasingly clear from many points of view that the Pomeranchon is a complicated object, and perhaps our prescription inevitably reflects this complication.

In addition to the results presented in this paper, the ABFST model can be used to make many detailed predictions concerning high-energy inelastic processes, only a few of which have been calculated so far. It will be of interest to examine the effects of off-shell continuation on these predictions, and to see if the use of DP form factors again leads to substantial improvements.

ACKNOWLEDGMENT

One of us (D.R.A.) wishes to thank Professor Geoffrey F. Chew for the hospitality of the theoretical group at the Lawrence Berkeley Laboratory.

APPENDIX

For the nonforward ABFST equation, it is convenient to introduce a function $B_{\ell,\lambda}(t; u, u')$ such that

$$B_{\ell,\lambda}(0; u, u') = A_{\lambda}(u, u') / (u' + m_{\pi}^2)^2. \quad (\text{A.1})$$

In terms of this function, the equation has the form^{13,14}

$$\begin{aligned} & [(u + m_{\pi}^2 - \frac{1}{4}t)^2 + ut(a_{\ell,\lambda}^2 + a_{\ell,\lambda-1}^2)] B_{\ell,\lambda}(t; u, u') \\ & + ut[a_{\ell,\lambda} a_{\ell,\lambda+1} B_{\ell,\lambda+2}(t; u, u') + a_{\ell,\lambda-1} a_{\ell,\lambda-2} B_{\ell,\lambda-2}(t; u, u')] \\ & = A_{\lambda}^R(t; u, u') + \frac{1}{16\pi^3(\lambda+1)} \int_0^{\infty} du'' A_{\lambda}^R(t; u, u'') B_{\ell,\lambda}(t; u'', u'), \end{aligned} \quad (\text{A.2})$$

where

$$\begin{aligned} a_{\ell,\lambda} &= \frac{1}{2} \left[\frac{(\lambda - \ell + 1)(\lambda + \ell + 2)}{(\lambda + 1)(\lambda + 2)} \right]^{\frac{1}{2}}, \quad \lambda \geq \ell; \\ &= 0, \quad \lambda < \ell; \end{aligned} \quad (\text{A.3})$$

and $A_{\lambda}^R(t; u, u')$ is related to the nonforward off-shell absorptive part $A^R(s, t; u, u')$ by the Laplace transformation given in Eq. (2.3). In writing Eq. (A.2) we have assumed that $A^R(s, t; u, u')$ remains fully $O(3,1)$ -symmetric at $t \neq 0$, and that the coupling between different values of λ arises only from the $O(3,1)$ symmetry breaking in the pion propagators. However, the general expression for the nonforward kernel, corresponding to Eq. (2.5) for the forward case, is

$$A^R(s, t; u, u') = 2\pi \sum_i \beta_i g_i^2 F_i^2(q_u) F_i(q_{\ell}) P_{J_i}(\cos \theta_s) \delta(s - m_i^2), \quad (\text{A.4})$$

where q_u (q_{ℓ}) is the c.m. momentum for the upper (lower) vertex on the right-hand side of Fig. 1:

$$q_{u,\ell} = \lambda^{\frac{1}{2}}(s, -u + \frac{1}{4}t \pm p \cdot k, -u' + \frac{1}{4}t \pm p \cdot k') / [2(s)^{\frac{1}{2}}], \quad (\text{A.5})$$

and $\cos \theta_s$ is the s-channel scattering angle:

$$\cos \theta_s = [\lambda(s, -u, -u') + st - (p \cdot k - p \cdot k')^2] / (4q_u q_{\ell} s). \quad (\text{A.6})$$

The terms $p \cdot k$ and $p \cdot k'$ in Eqs. (A.5) and (A.6) are clearly not $O(3,1)$ -invariant, and we have made the approximation of neglecting them. In the unmodified model for $J_1 = 0$ this makes no difference, because these terms do not appear in the on-shell kernel given by Eq. (2.10). For the off-shell continuation using DP form factors, the largest symmetry breaking in the kernel should arise from the factor $q_u q_{\ell} \cos \theta_s$ in the ρ resonance contribution. This factor gives rise to a finite number of nondiagonal terms on the right-hand side of Eq. (A.2), and we have made a numerical study of its effect. In Fig. 5 we show that this effect is small, although it is possible that the inclusion of all symmetry-breaking terms in the kernel might suffice to provide a tachyon-killing zero in the $I = 0$ residue function.

FOOTNOTES AND REFERENCES

- * Supported in part by the U.S. Atomic Energy Commission.
- + Participating guest, Lawrence Berkeley Laboratory; Fellow of the National Research Council of Argentina.
- † Present address: Cavendish Laboratory, Cambridge, England.
1. Don M. Tow, Phys. Rev. D2, 154 (1970).
 2. G. F. Chew, T. Rogers, and D. R. Snider, Phys. Rev. D2, 175 (1970).
 3. D. R. Snider and D. M. Tow, Phys. Rev. D3, 996 (1971).
 4. L. Caneschi and A. Schwimmer, Phys. Letters 33B, 577 (1970).
 5. A. Jurewicz et al., Nucl. Phys. B29, 269 (1971).
 6. L. Bertocchi, S. Fubini, and M. Tonin, Nuovo Cimento 25, 626 (1962); D. Amati, A. Stanghellini, and S. Fubini, ibid. 26, 896 (1962).
 7. L. W. Jones et al., Phys. Rev. Letters 25, 1679 (1970).
 8. B. R. Webber, Phys. Rev. Letters 27, 448 (1971).
 9. D. R. Avalos, Inclusion of the Pseudoscalar Model Octet in the ABFST Multiperipheral Model, Lawrence Radiation Laboratory Report UCRL-20810, May 1971, to be published in Phys. Rev. D.
 10. G. F. Chew and D. R. Snider, Phys. Rev. D1, 3453 (1970).
 11. H. P. Dürr and H. Pilkuhn, Nuovo Cimento 40A, 899 (1965).
 12. S. Nussinov and J. Rosner, J. Math. Phys. 7, 1670 (1966).
 13. V. Chung and D. R. Snider, Phys. Rev. 162, 1639 (1967).
 14. H. W. Wyld, Phys. Rev. D3, 3090 (1971); and CERN Report TH.1361, 1971 (unpublished).
 15. J. Dash, Cambridge Report DAMTP 71/19, 1971; D. Silverman and P. D. Ting, University of California (San Diego) Report UCSD-10F10-82, 1971 (unpublished).

16. E. Colton and P. E. Schlein, in Proceedings of the Conference on $\pi\pi$ and $K\pi$ Interactions, Argonne National Laboratory, 1969, edited by F. Loeffler and E. Malamud, p. 1; and references therein.
17. As quoted by P. E. Schlein, Ref. 16, p. 704.
18. G. Wolf, Phys. Rev. 182, 1538 (1969).
19. F. Bulos et al., Phys. Rev. Letters 26, 1453 (1971). See also the results of the Aachen-Berlin-CERN collaboration, J. Barsch et al., Nucl. Phys. B22, 1 (1970).
20. R. H. Dalitz, in High Energy Physics, edited by C. de Witt and M. Jacob (Gordon and Breach, New York, 1965), p. 299.
21. See for example J. Barsch et al., Nucl. Phys. B22, 109 (1970).
22. K. J. Foley et al., Phys. Rev. Letters 26, 413 (1971).
23. T. G. Trippe et al., Phys. Letters 28B, 203 (1968).

Table I. Assumed properties of low-energy resonances.

Resonance	Spin	Mass (GeV)	Full width (GeV)
ϵ	0	0.765	0.450
ρ	1	0.765	0.125
f	2	1.260	0.150
f'	2	1.514	0.073
g	3	1.670	0.170
ω	1	0.784	--- ^a
K^*	1	0.892	0.050
Φ	1	1.019	0.004
A_2	2	1.300	0.020
K^{**}	2	1.412	0.096

^a Contributes only as a bound state of KK .

Table II. Vertex parameters.

Vertex	Elasticity, x	R^2 (GeV ⁻²)	$\langle r^2 \rangle^{1/2}$ (F)
$\epsilon\pi\pi$	1.0	--- ^a	--- ^a
$\rho\pi\pi$	1.0	4.03	0.4
$f\pi\pi$	1.0	8.03	0.4
$f'\pi\pi$	0.1	11.90	0.4
$g\pi\pi$	0.92	11.90	0.4
ρKK	--- ^b	2.11	0.4
ωKK	--- ^b	2.14	0.4
ΦKK	0.8	2.77	0.4
$A_2 KK$	0.02	6.93	0.4
$f' KK$	0.8	7.56	0.4
$g KK$	0.08	10.71	0.4
$K^* K\pi$	1.0	1.30	0.3
$K^{**} K\pi$	0.5	3.51	0.3
$K^* K\eta$	--- ^b	2.10	0.4
$K^{**} K\eta$	0.02	6.82	0.4
$A_2\pi\eta$	0.16	6.05	0.4
$f'\eta\eta$	0.1	7.21	0.4

^a S-wave resonance.

^b Bound state.

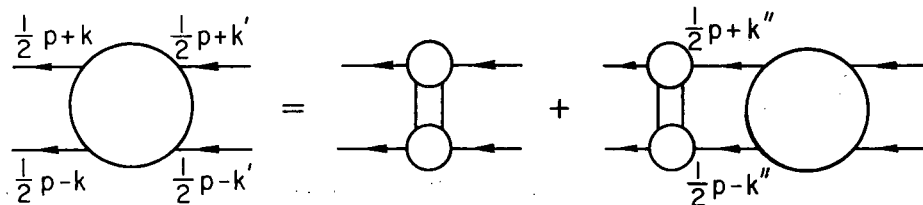
Table III. Results of this work. The first two columns give the intercepts of the $I = 0$ and $I = 1$ trajectories. The last column gives the coefficient of $\ln s$ in the average multiplicity ($\langle n \rangle = c \ln s + \text{const.}$).

	$\alpha_{I=0}(0)$	$\alpha_{I=1}(0)$	c
Experiment	0.7-1.0	0.5	1.02 ± 0.13^a
On-shell $\pi\pi$	0.30	0.14	0.74
Off-shell $\pi\pi$	0.57	0.36	0.84
Off-shell $\pi + K + \eta$	0.63	0.42	$\left\{ \begin{array}{l} 0.95 \\ \frac{\langle n_K \rangle}{\langle n_\pi \rangle} \sim 0.13 \end{array} \right.$

^a Reference 7.

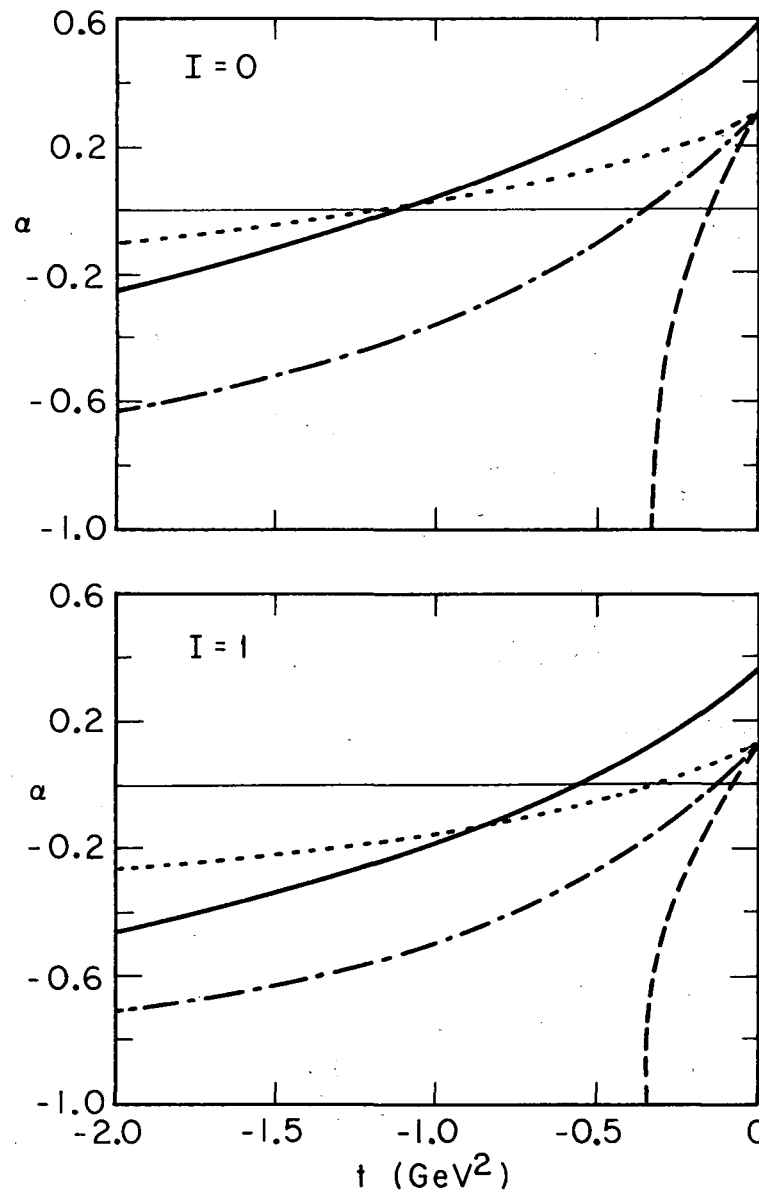
FIGURE CAPTIONS

- Fig. 1. The ABFST integral equation.
- Fig. 2. Leading output trajectories for the following parametrizations of the kernel: on-shell $\pi\pi$ amplitude (dashed curve); scalar resonances (dotted curve); off-shell $\cos \theta_s$ (dot-dashed curve); off-shell $\cos \theta_s$ with DP form factors (solid curve).
- Fig. 3. Residue functions for the output trajectories. The curves correspond to the various parametrizations described in the caption of Fig. 2.
- Fig. 4. The ABFST eigenfunctions when K and η exchange and DP form factors are included.
- Fig. 5. Effect of including the leading $0(3,1)$ -symmetry-breaking term in the ABFST kernel. The dashed and solid curves show the results obtained with and without inclusion of the term, respectively.



XBL 718-4086

Fig. 1



XBL718-4088

Fig. 2

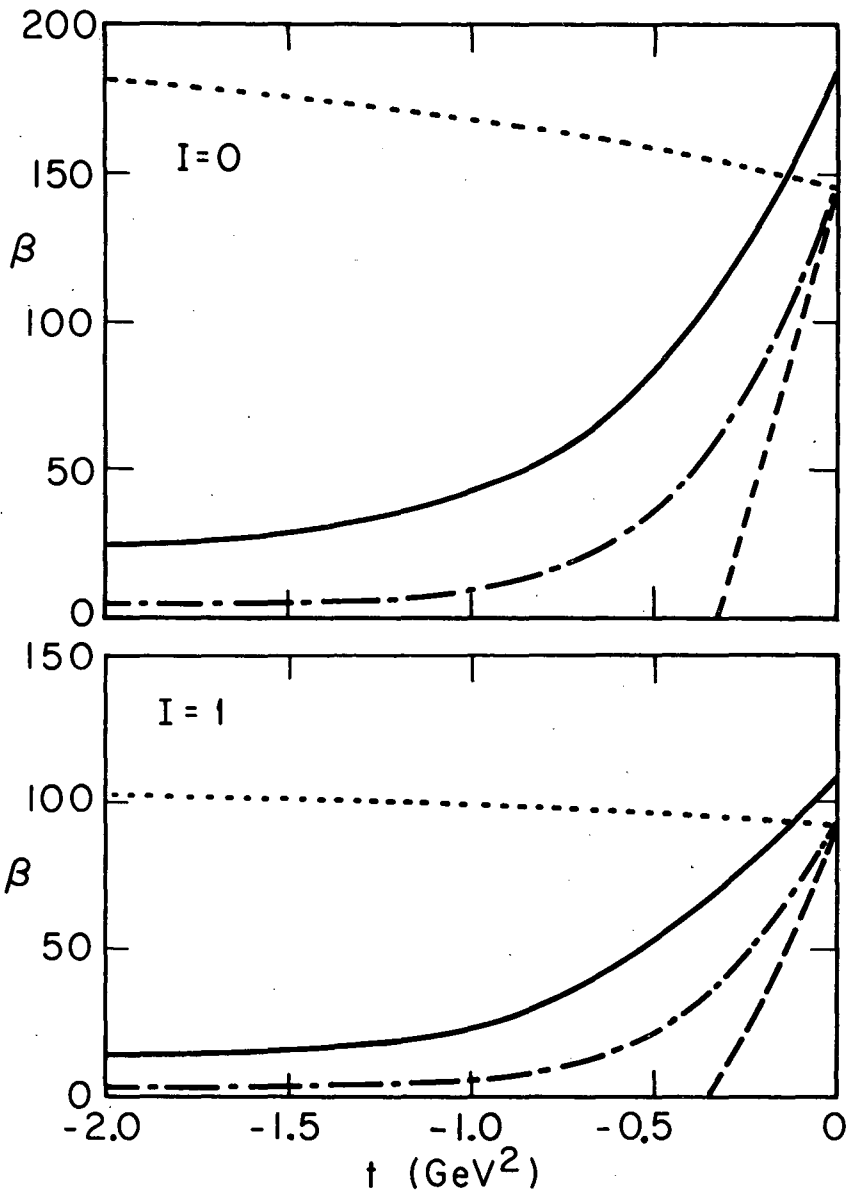


Fig. 3

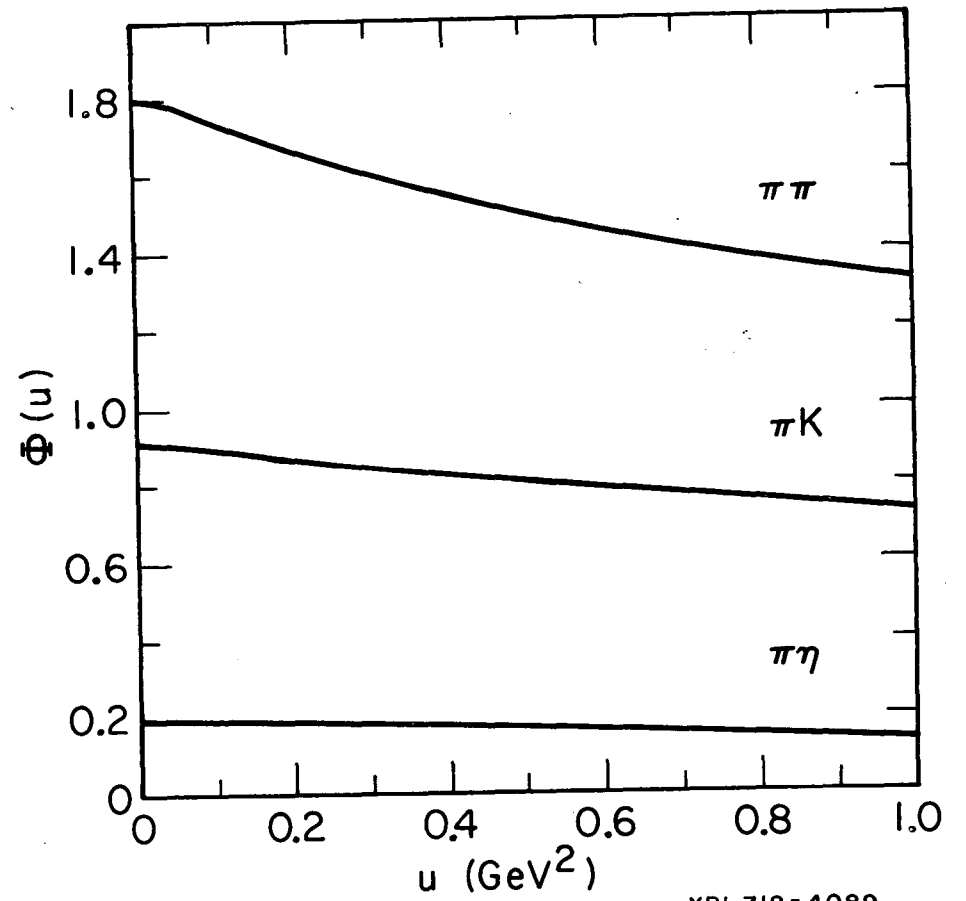
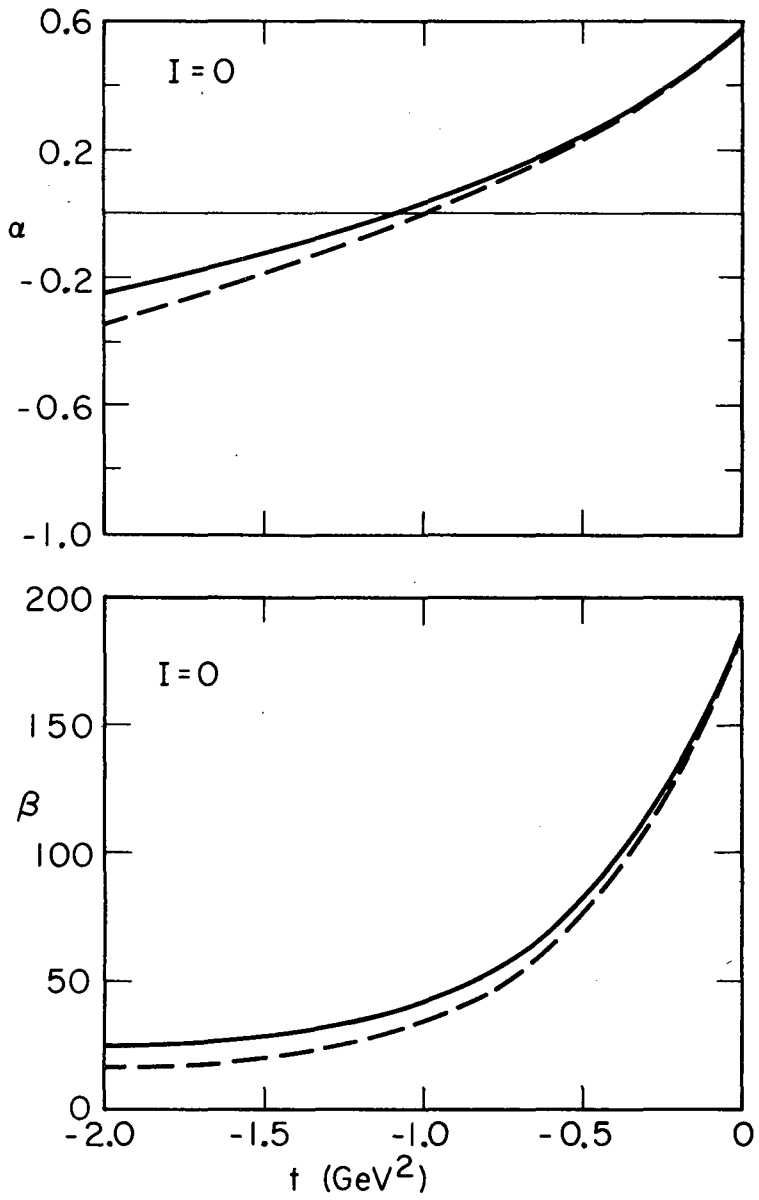


Fig. 4



XBL718-4090

Fig. 5

LEGAL NOTICE

This report was prepared as an account of work sponsored by the United States Government. Neither the United States nor the United States Atomic Energy Commission, nor any of their employees, nor any of their contractors, subcontractors, or their employees, makes any warranty, express or implied, or assumes any legal liability or responsibility for the accuracy, completeness or usefulness of any information, apparatus, product or process disclosed, or represents that its use would not infringe privately owned rights.

TECHNICAL INFORMATION DIVISION
LAWRENCE BERKELEY LABORATORY
UNIVERSITY OF CALIFORNIA
BERKELEY, CALIFORNIA 94720